

# Biofabrication



## PAPER

### OPEN ACCESS

RECEIVED  
21 July 2020

REVISED  
31 August 2020

ACCEPTED FOR PUBLICATION  
30 September 2020

PUBLISHED  
16 October 2020

Original content from this work may be used under the terms of the [Creative Commons Attribution 4.0 licence](#).

Any further distribution of this work must maintain attribution to the author(s) and the title of the work, journal citation and DOI.



# Direct extrusion of individually encapsulated endothelial and smooth muscle cells mimicking blood vessel structures and vascular native cell alignment

E Bosch-Rué<sup>1</sup> , Luis M Delgado<sup>1</sup> , F Javier Gil<sup>1</sup>  and Roman A Perez<sup>1,2</sup> 

<sup>1</sup> Bioengineering Institute of Technology (BIT), Universitat Internacional de Catalunya (UIC), Sant Cugat del Vallès, Spain  
<sup>2</sup> Author to whom any correspondence should be addressed.

E-mail: [rperezan@uic.es](mailto:rperezan@uic.es)

**Keywords:** blood vessel, tissue engineering, coaxial extrusion, vascular construct, cell-laden hydrogels

Supplementary material for this article is available [online](#)

## Abstract

Cardiovascular diseases (CVDs) are considered the principal cause of worldwide death, being atherosclerosis the main etiology. Up to now, the predominant treatment for CVDs has been bypass surgery from autologous source. However, due to previous harvest or the type of disease, this is not always an option. For this reason, tissue engineered blood vessels (TEBV) emerged as an alternative graft source for blood vessel replacement. In order to develop a TEBV, it should mimic the architecture of a native blood vessel encapsulating the specific vascular cells in their respective layers with native alignment, and with appropriate mechanical stability. Here, we propose the extrusion of two different cell encapsulating hydrogels, mainly alginate and collagen, and a sacrificial polymer, through a triple coaxial nozzle, which in contact with a crosslinking solution allows the formation of bilayered hollow fibers, mimicking the architecture of native blood vessels. Prior to extrusion, the innermost cell encapsulating hydrogel was loaded with human umbilical vein endothelial cells (HUVECs), whereas the outer hydrogel was loaded with human aortic smooth muscle cells (HASMCs). The size of the TEBV could be controlled by changing the injection speed, presenting homogeneity between the constructs. The obtained structures were robust, allowing its manipulation as well as the perfusion of liquids. Both cell types presented high rates of survival after the extrusion process as well as after 20 d in culture (over 90%). Additionally, a high percentage of HASMC and HUVEC were aligned perpendicular and parallel to the TEBV, respectively, in their own layers, resembling the physiological arrangement found *in vivo*. Our approach enables the rapid formation of TEBV-like structures presenting high cell viability and allowing proliferation and natural alignment of vascular cells.

## 1. Introduction

As reported by the World Health Organization (WHO), 31% of global death is due to cardiovascular diseases (CVDs), considered the principal cause of worldwide death [1]. The main etiology of CVDs is the narrowing and occlusion of blood vessels as a result of atherosclerotic plaque formation in the inner layer of arteries, known as atherosclerosis, which impedes the blood flow and eventually leads to tissue ischemia [2]. Up to now, the gold standard strategies to treat CVDs have been the use of stents or blood vessel replacement by bypass surgery. The use of

stents can induce endothelial damage triggering a cascade of events that leads to the re-narrowing of the vessel, known as restenosis [3]. Although stents have been improved over time to reduce restenosis [4], it still remains a problem in clinical practice [5]. The alternative strategy for blood vessel replacement generally considers autologous source, such as saphenous vein or mammary artery [6, 7]. However, because of the inherent disease of the patient or due to previous harvest, the autologous source offers a limited solution. The use of decellularized xenogeneic vessels has also been proposed to surpass this problem, and also because they can preserve the

extracellular matrix (ECM) of native vessels allowing cell migration, proliferation and survival. However, the complete removal of immunogenic molecules still remains a challenge and can trigger an immune response [8]. Due to the aforementioned issues, significant efforts are steering in developing tissue engineered blood vessels (TEBV) as an alternative graft source for bypass surgery.

To bioengineer a TEBV, it is important to mimic to the highest extent the architecture and the structural components of a blood vessel. Higher caliber vessels, such as arteries, are composed of two main functional layers: tunica intima and tunica media. Tunica intima is the closest to the blood and it is comprised of a confluent monolayer of endothelial cells (ECs) aligned in the direction of the blood flow [9]. Tunica media is composed of smooth muscle cells (SMCs) which are concentrically arranged, being rich in collagen type I and elastin. Several mechanical functionalities of the blood vessel, such as the vasoactivity (contraction and dilation) are mainly related with SMCs alignment [10, 11] and for this reason, special attention is focused in achieving a proper alignment of these cells when developing a TEBV. Therefore, as a first step to develop a TEBV, the earliest achievements to accomplish in vascular engineering should be: (i) proper mechanical stability of the construct to allow handling and perfusion; (ii) obtaining a multilayered structure resembling the native arrangement; (iii) the allocation of vascular specific cell types in their respective layer, with a proper ECM allowing their survival; (iv) and concentric orientation of SMCs.

To achieve mechanical stability of the constructs, the use of synthetic biodegradable polymers has been proposed due to their inherent mechanical properties. In general, these synthetic polymers present adequate mechanical properties but limited biological activity. A commonly used method using synthetic materials is sheet rolling, that uses a biomaterial sheet on top of which ECs and/or SMCs can be seeded. The sheet is then rolled over a mandrel to form a tubular structure [12], with the possibility to form more than one layer [13]. To further guide cells and orientate them on the desired direction, surface patterning can be performed either by lithography based techniques or by electrospinning [14]. Actually, the latter technology itself can be used to obtain tubular constructs by simply electrospinning onto small rotating mandrels [15], where SMCs are seeded on the top of the construct and ECs in the inner surface. Using both approaches, it takes several steps and time to obtain a vascular construct, especially with sheet rolling, as cells have to be seeded on the surface of 2D biomaterial and allow their proliferation [12], before rolling it to obtain a tubular structure. Furthermore, the released products from synthetic materials degradation have been shown to alter the contract phenotype of SMCs [16].

For this reason, alternative materials and technologies are needed to provide a more natural environment for cells, that allows forming layered structures incorporating different cell types with enough mechanical stability. For this purpose, extrusion based system of natural materials, with concentric nozzles has recently shown interesting results, allowing the fabrication of core shell layered fibers in a one step process [17]. This core-shell technology has allowed the encapsulation of cell types in the inner layer, being sheathed by an acellular hydrogel layer, generally alginate, as it provides mechanical stability [18]. Despite these systems may eventually allow the encapsulation of cells in different compartments, their use as a blood vessel is very limited due to the absence of the lumen. To further mimic a blood vessel, other studies have incorporated a water soluble polymer in the inner layer to obtain a hollow fiber, allowing the encapsulation of vascular related cells on the outer layer [17, 19]. The main limitation of this system is the limited functionality due to the presence of one individual layer where cells can be placed. However, a recent study was able to proof functionality of these TEBVs structures encapsulating both EC and SMCs in different layers [20]. Conversely, an added value of the extrusion based process is the ability to align cells based on the shear stress applied, avoiding the use of patterning and electrospinning techniques. In a previous study, alignment of mesenchymal stem cells (MSCs) was demonstrated due to the shear stress during extrusion [21]. Moreover, it is described that the shear stress of the blood flow can induce the parallel alignment of EC [22], and SMCs can be aligned in a shear-stress dependent manner [23], being perpendicular with low shear stress. Therefore, the shear stress generated during the extrusion process might induce a specific cell alignment.

Here, we aim at using a triple concentric nozzle to form dual-layered blood vessel-like structure encapsulating human umbilical vein endothelial cells (HUVECs) and human aortic smooth muscle cells (HASMCs) in their respective layers. Furthermore, we expect that the shear stress applied during the extrusion based process will allow the alignment of HUVECs parallel to the direction of the TEBV whereas HASMCs will align perpendicular to the TEBV. To the best of our knowledge, this is the first attempt to extrude at the same time a multilayered tubular structure with both cell types in their respective layers to form a blood vessel-like structure while maintaining its native cell alignment provided by the environmental factors.

## 2. Material and methods

### 2.1. Collagen type I isolation

Collagen type I was isolated from bovine tendons obtained from an abattoir and all the isolation process was based on well-established protocols [24].

First, tendon was separated from the surrounding fascia and was cut to small pieces with the aid of a blender, followed by three washes with phosphate buffered saline (PBS). Then, the sliced tendon was dissolved with 1M acetic acid under agitation for 72 h. Enzymatic digestion was performed using porcine gastric mucosa pepsin (Sigma) at 40 U mg<sup>-1</sup> of tendon under stirring, 2 h at room temperature (<20 °C) and 72 h at 4 °C. The resultant enzymatic digestion was filtered to obtain pepsin soluble collagen and was purified by salt precipitation (0,9M NaCl) during 24 h. The precipitated collagen was collected and dissolved with 1M acetic acid under stirring for 5 d. Finally, collagen solution was dialyzed (MW 8000 cut off) repeatedly against 1 mM acetic acid and the dialyzed collagen solution was kept at 4 °C. Collagen concentration was determined using dry weight ( $\approx 5.7$  mg ml<sup>-1</sup>) and collagen purity was evaluated using sodium dodecyl sulfate polyacrylamide gel electrophoresis (SDS-PAGE) followed by Coomassie staining (see supplementary information-figure 1(<https://stacks.iop.org/BF/13/015003/mmedia>)).

## 2.2. Cell culture

Human umbilical vein endothelial cells (HUVECs) (Lonza) and HASMCs (ATCC) were used. For cell expansion, HUVEC were seeded at a density of 2500 cells/cm<sup>2</sup> with endothelial growth medium-2 bulletkit (EGM-2) (Lonza) containing VEGF, rhFGF-B, rhEGF, r-IGF-1, hydrocortisone, ascorbic acid, gentamicin sulfate, amphotericin-B and 2% of FBS. HASMC were seeded at a density of 2500 cells cm<sup>-2</sup> with vascular cell basal medium supplemented with vascular smooth muscle cell growth kit (ATCC) containing 5 ng ml<sup>-1</sup> rh-FGF-basic, 5  $\mu$ g ml<sup>-1</sup> rh-Insulin, 50  $\mu$ g ml<sup>-1</sup> ascorbic acid, 10 mM L-glutamine, 5 ng ml<sup>-1</sup> rh EGF, 5% FBS and 1% Penicillin-streptomycin. When both cell types reached 70%–85% confluence, they were passaged using 0,25% Trypsin-EDTA (Gibco) or they were ready to be used for TEBV development. All cells were cultured in standard cell culture conditions (37 °C and 5% CO<sub>2</sub>).

## 2.3. Endothelial cell encapsulation in core-shell fibers

The methodology to obtain a core-shell fiber was followed from a previous study [21]. Briefly, a dual concentric nozzle (23G inner and 17G outer, NanoNC) was used to obtain a core-shell fiber in which two different biomaterials were extruded: alginate (Panreac Applichem) at a ratio of 1,5% (%wt) in the outer layer and 2 mg ml<sup>-1</sup> of collagen type I in the core. The concentric flows were extruded at 50 ml h<sup>-1</sup> into a 150 mM calcium chloride (CaCl<sub>2</sub>) (Sigma) solution and incubated for 5 min. After that, fibers were rinsed with H<sub>2</sub>O miliQ. In order to verify if our initial hypothesis was viable, allowing the alignment of HUVEC

on the direction of a core shell fiber as we previously observed with mesenchymal stem cells [21], a small preliminary experiment was performed. Furthermore, due to the higher sensitivity of HUVEC compared to MSC, we also aimed exploring if cell concentration could have an effect on cell alignment and survival as well as to verify if the shear stress caused during the extrusion process could jeopardize cell viability. Different amounts of HUVEC ( $1 \times 10^5$ ,  $1 \times 10^6$  and  $2 \times 10^6$  cells ml<sup>-1</sup>) were loaded in the core with collagen type I. After the incubation with 150 mM of CaCl<sub>2</sub>, three washes with fresh cell culture media were performed to remove the excess of calcium and, finally, they were cultured with EGM-2 medium (Lonza) up to 7 d and optical images were acquired.

## 2.4. Core-shell hollow fiber fabrication

To develop a dual layer hollow fiber as a tissue engineered blood vessel (TEBV) structure, a triple concentric nozzle (23G outer, 17G middle and 13G inner) (NanoNC) was used. Schematic representation of the method is shown in figure 1. The nozzle was fed with the help of injection pumps with three different materials placed in syringes to allow the formation of the tri-concentric fiber. The inner syringe was loaded with a 25% wt Pluronic F-127 (Sigma) aqueous solution, as a sacrifice material. The middle syringe was loaded with the previously extracted collagen type I. In order to maximize the stability of the tubular structure, different collagen concentrations ranging from 2 to 5 mg ml<sup>-1</sup> were tested. To mimic the native conditions of blood vessels and to present an adequate environment for cell survival, collagen was self-assembled by adding 200  $\mu$ l of 10x PBS and the necessary amount of NaOH, 1M or 5M, was added to 2 ml of collagen. The outer syringe was loaded with a mix of sodium alginate (A3249, Panreac Applichem) and collagen type I. In this case, the concentration of each hydrogel was optimized by maximizing the collagen presence without jeopardizing the mechanical stability of the fiber provided by the alginate. The injection speed was varied between 25 and 50 ml h<sup>-1</sup> to study the effect of the injection speed on the general parameters of the blood vessel like structure, mainly shell thickness and fiber size. All the loaded syringes were kept at 4 °C. The tip of the nozzle was placed in contact with a 150 mM calcium chloride bath at 37 °C, where calcium allowed an instant crosslinking of the outer layer containing alginate, providing stability to the fiber structure, whereas the increased temperature allowed collagen self-assembling contributing to the stabilization of both the outer and middle layer. The tri-layered structures were maintained in the crosslinking solution during 10–15 min. After collagen gelation, the tri-layered fiber was placed in H<sub>2</sub>O miliQ and was cut to a length of 1 cm. Pluronic was removed from the inner core by dissolution with H<sub>2</sub>O miliQ during

5 min, obtaining the TEBV structure. The outer and the inner diameter of TEBV were measured for each injection speed. Additionally, manual perfusion with red food ink was performed to confirm the hollow structured vessel and to qualitatively assess the sufficient mechanical stability of the vessel to withstand perfusion of liquids without bursting the structure or leaking the perfused liquids.

### 2.5. Individual cell encapsulation within tissue engineered blood vessel structures (TEBV)

Initially, in order to assess the individual behavior of each cell type encapsulated within its designated compartment, hollow fibers encapsulating HUVEC or HASMC were prepared. All the procedure was performed under sterile conditions. Pluronic and sodium alginate powders were sterilized with UV. Then, they were mixed with sterile milli-Q water to achieve 25 and 5% (% wt) of Pluronic and alginate, respectively. For the encapsulation of cells, the previously described procedure was followed using  $50 \text{ ml h}^{-1}$  as the injection speed. For TEBV containing only HUVEC (TEBV-HUVEC), a small volume of culture media containing  $15 \times 10^6$  HUVEC cells/ml was loaded in the collagen syringe after pH neutralization. Based on our preliminary results, this cell concentration was used to achieve, within the middle layer, at least a continuous cell monolayer that would allow a continuous endothelial cell layer that would mimic the native structure of blood vessels. For TEBV containing only HASMC (TEBV-HASMC), 2 ml of 5% alginate and 3 ml of  $5 \text{ mg ml}^{-1}$  of collagen (previous neutralized) were mixed to achieve a final concentration of 2% and  $3 \text{ mg ml}^{-1}$  of alginate and collagen, respectively. Then, a small volume of HASMCs was added achieving a final concentration of  $10 \times 10^6$  cells  $\text{ml}^{-1}$ . It is worth to mention that the different concentration of HUVEC and HASMCs used is due to their different size, being HUVEC about three times smaller than HASMCs [25]. As HASMCs have more matrix to proliferate and based on a previous study where  $10 \times 10^6$  HASMCs/ml were used demonstrating the ability to cover TEBV wall [26], we used the final ratio of HUVEC:HASMCs of 3:2, avoiding at the same time an initial high HASMC confluence to allow proper cell alignment. Once complete crosslinking of alginate and gelation of collagen was achieved, the TEBVs were rinsed three times with fresh cell culture medium to remove the excess of  $\text{CaCl}_2$ . Then, TEBV were cut to a length of 1 cm and, finally, each cell type was cultured with each specific cell culture medium mentioned.

### 2.6. Co-encapsulation of HUVEC and HASMCs within tissue engineered blood vessel structures (TEBV)

For the co-culture assay (TEBV-co), HUVEC were loaded into the collagen syringe (middle layer) and HASMC were loaded into the alginate mixed with

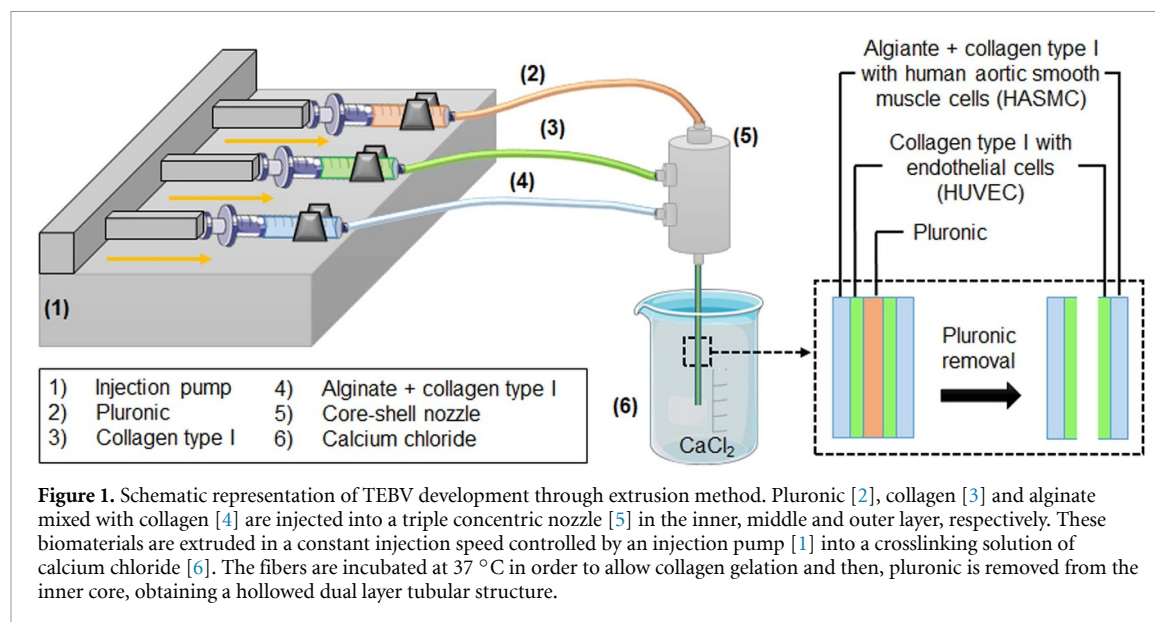
collagen syringe (outer layer), following a similar cell encapsulation method as the one performed for individual cell encapsulation. In a similar way, after alginate crosslinking and collagen gelation, the TEBVs were rinsed three times with fresh cell culture medium to remove the excess of  $\text{CaCl}_2$ . Then, TEBV were cut to a length of 1 cm and 50% of each cell culture media was used (both cell types proved to survive and proliferate, see supplementary information—figure 2).

### 2.7. Cell viability analysis

The cell viability of HUVEC, HASMC or both in co-culture was assessed at 24 h, to quantitatively assess cell survival after the shear stress produced by the extrusion method, and at 20 d, to prove if cells could survive after a long cell culture period within the TEBV structure. The LIVE/DEAD cell imaging kit (Invitrogen) was used following manufacturer's instructions. Briefly, the methodology consists of a live component which stains live cells giving a uniform green fluorescence (excitation/emission wavelengths were 488/515 nm) and a dead component which stains death cells producing a nuclear red fluorescence (excitation/emission wavelengths were 570/602 nm). Equal volumes of both components were added in the cell culture medium with TEBVs reaching a final concentration of  $1 \times$ . After 15 min of incubation protected from light, cells were imaged with a laser scanning confocal microscope (Leica SP8, LAS X software version 3.5.5.19976). As a positive control for cell death, some TEBV were previously treated with 4% PFA at room temperature during 30 min followed by an incubation with  $1 \times$  PBS/0,5% triton X-100 during 10 min. Three samples per time point were analyzed and three captures at different heights per sample were acquired. Images were analyzed using ImageJ software (ImageJ 1.52a) and live and dead cells were counted for each one. Viability was calculated as number of live cells divided per total number of cells (live and dead), as a percentage.

### 2.8. Cell proliferation assay

To assess the proliferation of cells, quantification of double-stranded DNA (dsDNA) using fluorimetric dsDNA quantification kit (Quant-It Picogreen dsDNA assay Kit, Invitrogen) was performed according manufacturer's instructions. Time points were at 0, 2, 5, 12 and 20 d for TEBV-HUVEC and TEBV-HASMC and at 0, 2, 8, 12 and 20 d for TEBV-co. Because there was not a big difference between day 2 and 5 when cells were cultured separately, we decided to assess it at day 8 in co-culture conditions instead of day 5. Three samples per time point were analyzed. Briefly, each sample was collected with  $100 \mu\text{l}$  of  $1 \times$  Tris-EDTA (TE) buffer and submitted to a three cycles of freezing and defrosting to lyse the cells. Between cycles, samples were mechanically disrupted by pipetting to allow the release of



DNA from TEBV structures. After spin centrifugation, 100  $\mu\text{l}$  of the supernatant was transferred into an opaque 96-well plate and mixed with 100  $\mu\text{l}$  of diluted Picogreen (1:200). The plate was incubated 5 min at room temperature protected from light. Then, samples were excited at 480 nm and fluorescence intensity was measured at 520 nm using a spectrofluorometer (Synergy H1 microplate reader, BioTek). A standard curve was plotted using  $\lambda$  DNA standard from 0 to 1000  $\text{ng ml}^{-1}$  and DNA amount of the samples were calculated from the standard curve.

### 2.9. Cell morphology of individual cell encapsulation and alignment

In order to assess the organization and alignment of cells in TEBV-HUVEC and TEBV-HASMC, actin filaments (F-actin) were stained with phalloidin (Acti-stain 488 fluorescent phalloidin, Cytoskeleton, Inc) at the end of experiment, day 20, and at earlier time points, day 9 for HASMC and day 16 for HUVEC. Briefly, TEBV were rinsed with PBS prior the fixation with 4% PFA during 20 min at room temperature. After three washes of PBS, TEBV were permeabilized with 0,5% Triton-100x/PBS for 10 min. Afterwards, TEBV were rinsed three times with PBS and then incubated at room temperature with 100 nM Acti-stain 488 phalloidin protected from light for 30 min. Upon PBS washing, samples were incubated with DAPI (NucBlue Fixed Cell stain DAPI, LifeTechnologies) for 5 min. Finally, samples were kept with PBS and visualized by confocal laser microscopy (Leica SP8, LAS X software version 3.5.5.19976) (excitation/emission wavelengths were 480/520 nm for phalloidin and 405/460 for DAPI). Images processing and 3D reconstruction were performed with IMARIS software (Imaris 8.2, Bitplane and Oxford Instruments).

The alignment of HASMC was assessed measuring the alignment of actin filaments using the freely OrientationJ plugin for Fiji/ImageJ, based on the analysis of pixel-by-pixel vector field from the intensity gradient in the vertical and horizontal directions of the image, as further detailed in <http://bigwww.epfl.ch/demo/orientation/> [27]. Different representative regions of different TEBV were analyzed, analyzing eight images with a minimum of 700 cells/image. The percentage of alignment between  $|0 \pm 45^\circ|$  and  $|90 \pm 45^\circ|$  was calculated for each time point as a way to quantify the parallel alignment of HUVEC and perpendicular and diagonal alignment of HASMC within TEBV, respectively.

### 2.10. Cell morphology of co-cultured encapsulated cells in tissue engineered blood vessels (TEBV)

Finally, in order to understand if the co-culture would disrupt the cell morphology as well as if the cells could be allocated on their respective compartments, each cell type was stained with different colored cell tracker fluorescence probes previous the development of TEBV structures. HUVEC cells were stained with Green CMFDA (Invitrogen) and HASMC were stained with Red CMTPIX (Invitrogen), emitting a green and red signal, respectively. Each cell tracker was added in the specific cell culture media at a final concentration of 10  $\mu\text{M}$  and incubated with cells during 45 min at 37 °C in 5%  $\text{CO}_2$  protected from light. After incubation, cells were detached with Trypsin-EDTA (Gibco), centrifuged at 150xg for 3 min and used for blood vessel formation. Once TEBV were developed, they were imaged at 5 d by a confocal laser microscopy (Leica SP8, LAS X software version 3.5.5.19976). The excitation/emission wavelengths were 492/517 for Green CMFDA and 577/602 for Red CMTPIX. Images were processed and

3D reconstruction was performed with IMARIS software (Imaris 8.2, Bitplane and Oxford Instruments).

### 2.11. Statistical analysis

Statistical analysis was performed using SPSS software (SPSS v21, IBM). Kruskal-Wallis and Mann Whitney U non parametric tests were used to compare the diameters of the TEBV at different injection speeds (data represented as mean  $\pm$  standard deviation;  $n = 10$ ) and the DNA amount of cells at different time points (values of all time points were compared to day 0) ( $n = 3$ ). P-value of less than 0.05 was considered statistically significant.

## 3. Results

### 3.1. Development of acellular TEBV-like structure

Maintaining a tubular structure is one of the first requisites to develop a TEBV-like structure. Experiments showed that the best conditions to maintain a tubular conformation were: 5 mg ml<sup>-1</sup> of collagen in the middle layer, which could maintain the structure once Pluronic was removed (figures 2(A)); and a final concentration of 2% of alginate and 3 mg ml<sup>-1</sup> of collagen in the outer layer, in which HASMC stretching and orientation was observed (supplementary information—figure 3). These conditions allowed a stable dual-layered tubular construct that could easily be handled (see supplementary information—video 1).

Results showed a direct relation between the injection speed and the diameter of the construct, showing smaller diameters of the TEBV-like structures with the lower injection speed (figure 2(B)). The outer and inner diameter were 1683.5  $\pm$  45.7  $\mu$ m and 1453.7  $\pm$  55.8  $\mu$ m for 50 ml h<sup>-1</sup> and 1474.3  $\pm$  60.4 and 1286.7  $\pm$  61.6  $\mu$ m for 25 ml h<sup>-1</sup>, being statistically significant the differences between the two injection speeds ( $p < 0.01$ ). The wall thickness was 114.9  $\pm$  13.7  $\mu$ m and 93.8  $\pm$  10.5  $\mu$ m for 50 and 25 ml h<sup>-1</sup> respectively, also presenting statistically significant differences between them ( $p < 0.01$ ). It is also worth highlighting the low variability in the different measurements, which are related with the fabrication of homogenous sized TEBVs.

Furthermore, the openness of TEBV-like structures and its perfusion was assessed using manual perfusion with red food ink, demonstrating a free flow through de TEBV, as shown in figure 2(C) and in the video (see Supplementary Information—Video 2).

### 3.2. Proof of concept: alignment of HUVEC cells

A preliminary study was performed to validate if HUVEC cells were able to align into the longitudinal core-shell fiber axis. figure 3 displays representative phase contrast microscope images of HUVEC during culture for up to 3 d when encapsulated within core-shell collagen-alginate fibers. First of all,

the lowest cell density (1x10<sup>5</sup> cells ml<sup>-1</sup>) induced large zones without cells which maintained the rounded morphology overtime. Although this large zones without cells were smaller for the intermediate cell density (1x10<sup>6</sup> cells ml<sup>-1</sup>), HUVEC cells maintained rounded morphology with negligible cell-to-cell interaction. Nevertheless, the highest cell density (2x10<sup>6</sup> cells ml<sup>-1</sup>) induced reduction of distance between cells at day 0 and cell spreading at day 3, as shown in figure 3. Moreover, HUVEC cells were aligned parallel to the core-shell fiber with the highest cell density at day 3.

### 3.3. Proliferation and viability of individual HUVEC and HASMC encapsulation within tissue engineered blood vessels (TEBV)

After the preliminary results, in which the non-hollowed core shell fibers proofed the alignment of HUVEC on the direction of the fiber as well as the need to encapsulate high cell density within the fibers, we proceeded to encapsulate the cells in the hollowed TEBV-like structure. The encapsulation of HUVEC in the middle layer (TEBV-HUVEC) resulted in HUVEC stretching within 24 h, mostly with a parallel alignment and practically covering the entire core with a monolayer within 2 d (figure 4(A)). A significant increase of DNA content arising from HUVEC was observed between day 0 and day 2 ( $p < 0.05$ ), remaining stable for the rest of the time points suggesting that HUVEC could proliferate within TEBV-like structure and that they reached confluence at day 2 (figure 4(B)). Furthermore, live/dead assays revealed higher rates of cell survival, being near to 95% at 24 h and 20 d (figure 4(C)).

When HASMC were encapsulated in the outer layer (TEBV-HASMC), cells started to lengthen at day 2 and covered the tubular wall structure at day 13 showing signs of perpendicular alignment respect TEBV direction (figure 5(A)). There was a significant gradual increase of the DNA content from HASMC that could be observed at all time points compared to day 0 ( $p < 0.05$ ), suggesting that these cells could also proliferate within the construct (figure 5(B)). Similar to HUVEC, HASMCs showed high rates of cell survival after 24 h and 20 d, being close to 95% in both cases.

### 3.4. Organization and alignment of HUVEC and HASMC when encapsulated individually in tissue engineered blood vessel (TEBV) structures

In order to confirm the homogenous coverage of each individual cell type within the blood vessel like structure, a 3D reconstruction with phalloidin and DAPI was performed. Until day 16, TEBV-HUVEC formed a monolayer (figure 6(A)), but at the final time point, cells reorganized over it (figures 6(B) and (C)). Unlike HUVEC, HASMC could proliferate forming a dense layer observed from day 9 (figure 6(D)) to

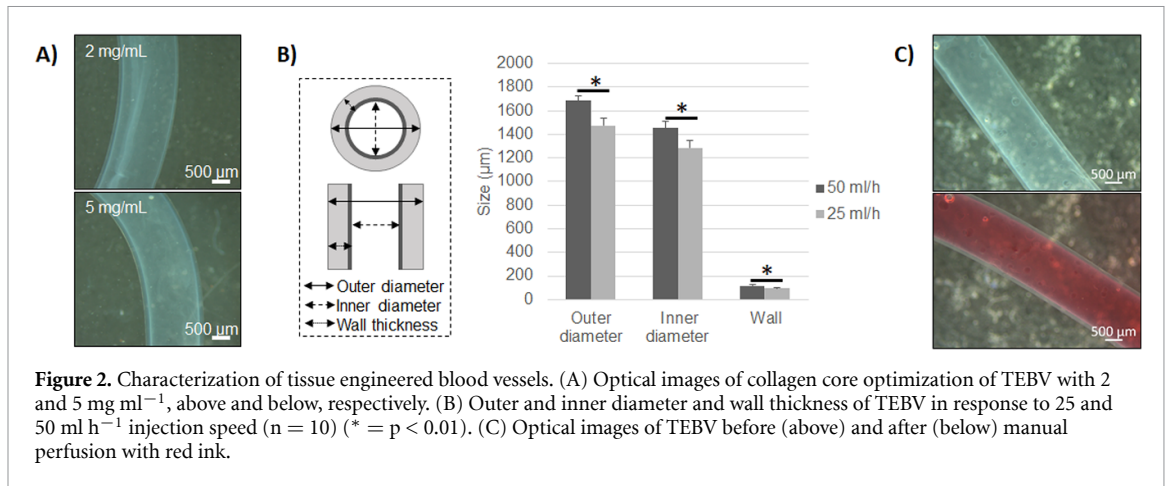


**Figure 2.** Characterization of tissue engineered blood vessels. (A) Optical images of collagen core optimization of TEBV with 2 and 5  $\text{mg ml}^{-1}$ , above and below, respectively. (B) Outer and inner diameter and wall thickness of TEBV in response to 25 and 50  $\text{ml h}^{-1}$  injection speed ( $n = 10$ ) (\* =  $p < 0.01$ ). (C) Optical images of TEBV before (above) and after (below) manual perfusion with red ink.

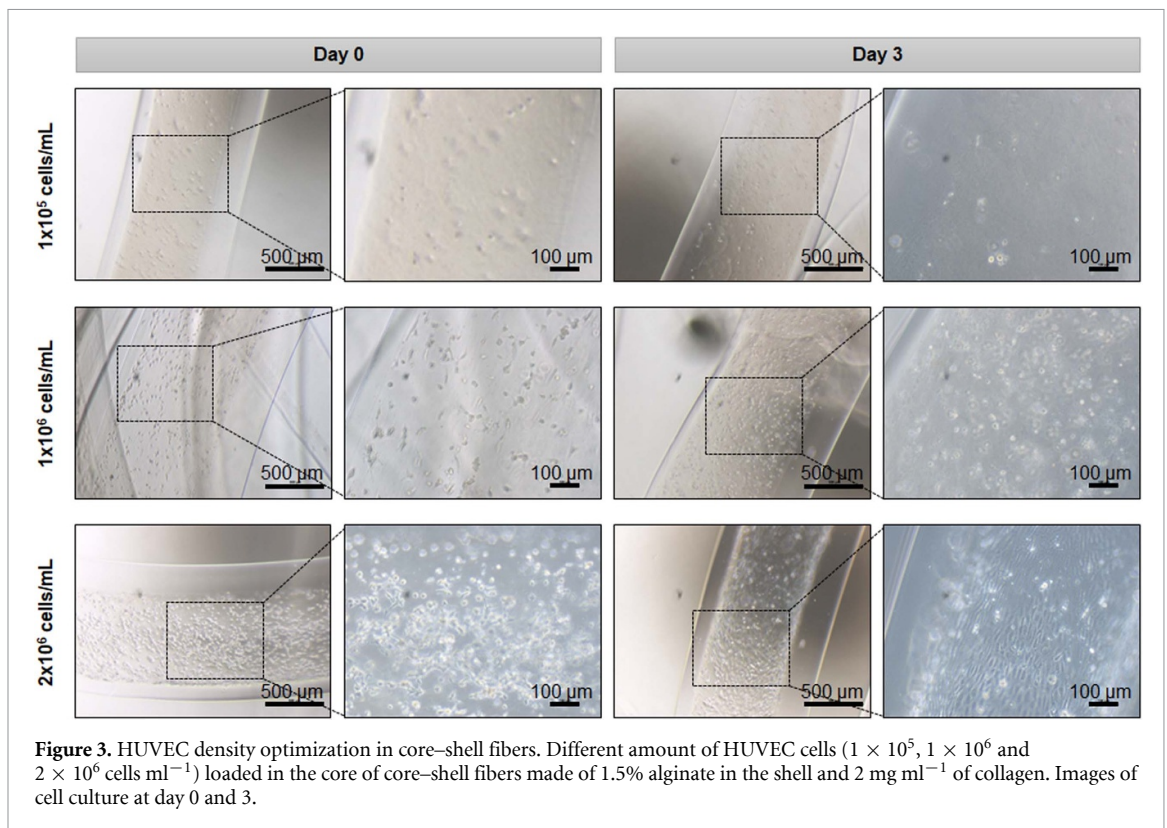


**Figure 3.** HUVEC density optimization in core-shell fibers. Different amount of HUVEC cells ( $1 \times 10^5$ ,  $1 \times 10^6$  and  $2 \times 10^6$   $\text{cells mL}^{-1}$ ) loaded in the core of core-shell fibers made of 1.5% alginate in the shell and 2  $\text{mg ml}^{-1}$  of collagen. Images of cell culture at day 0 and 3.

day 20 (figures 6(E) and (F)). Cell alignment analysis showed 74% and 17% of HUVEC cells aligned between 0 and  $45^\circ$  respect to TEBV direction at day 16 and 20, respectively (figures 7(A)–(D)). The reduction of a more parallel alignment might be due to the reorganization of cells over the monolayer and the difficulty to analyze the cells that were below it. The alignment of HASMC between  $45$  and  $90^\circ$  respect the direction of TEBV was 73% and 51% at day 9 and day 20, respectively (figures 8(A)–(D)). This diagonal-perpendicular alignment was consistent with the optical microscope images of TEBV-HASMC and (figures 5(A) and 3(D)) reconstruction with phalloidin (figures 6(D)–(F)), resembling natural alignment of native vessels. The trend in cell alignment showed for the different TEBV was consistent for the different constructs fabricated, showing that all the TEBV presented the described alignment.

### 3.5. Co-culture within TEBV-like structure

The following step was to assess the behavior of HUVEC and HASMC once they were co-cultured within TEBV-like structure (TEBV-co). The live/dead assay confirmed high cell viability at 24 h and at 20 d, showing over 96% and 94%, respectively (figure 9(A)). However, the amount of DNA remained constant until day 12, followed by a moderate increase in DNA content ( $p < 0.05$ ) (figure 9(B)).

Optical microscope images showed stretched cells in the inner layer at day 2 and stretched cells in the outer layer from day 12 (figure 9(C)). Visualizing the different cell types in co-culture was difficult with optical microscopy as well as with phalloidin and DAPI staining. Therefore, cells were stained with cell trackers in order to identify the two different cell types. At day 5, HUVEC were

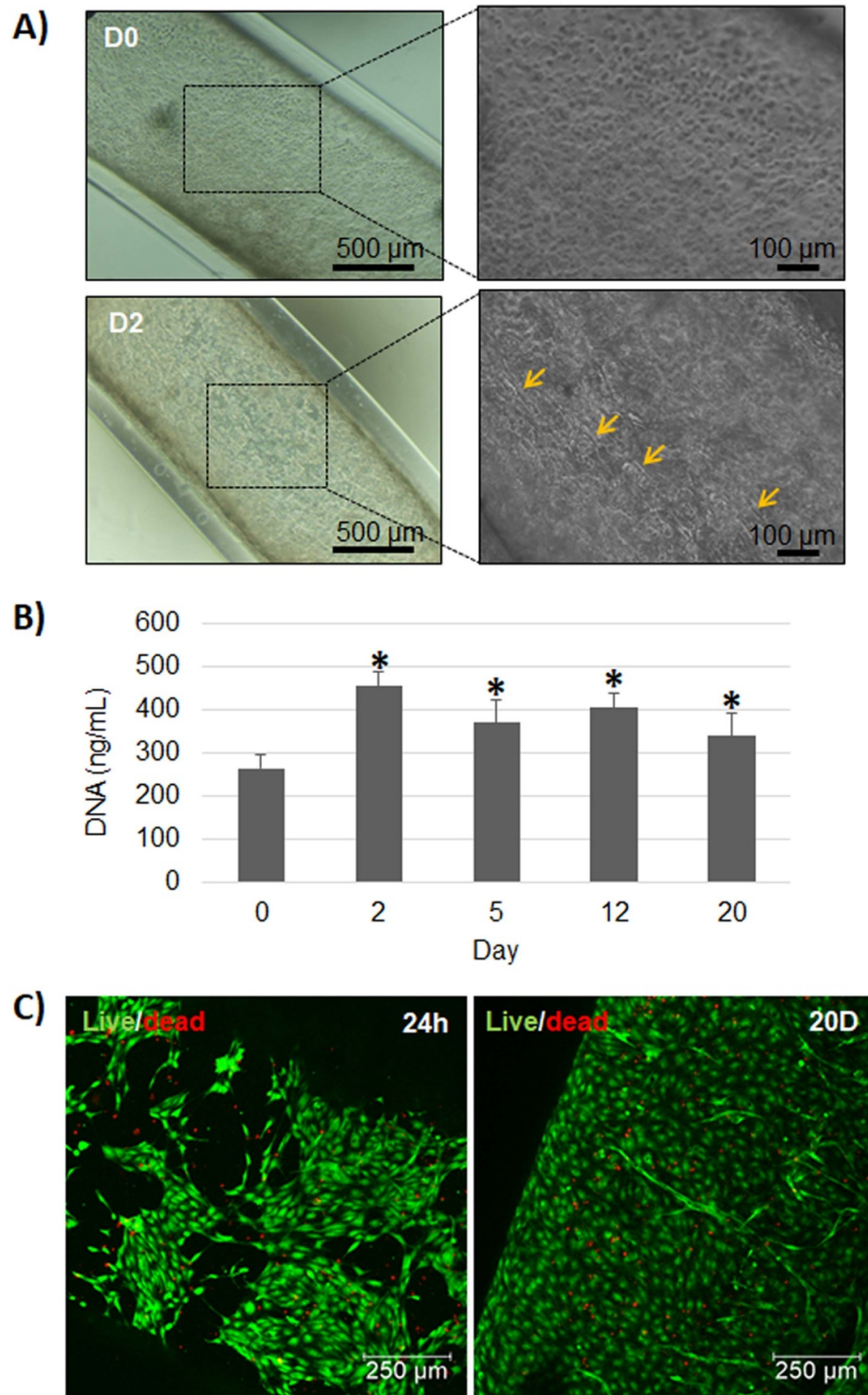


**Figure 4.** Encapsulation of HUVEC in TEBV (TEBV-HUVEC). (A) Optical microscope images of TEBV with HUVEC in the core at day 0 and 2. Arrows indicate some aligned cells. (B) HUVEC DNA content in TEBV at day 0, 2, 5, 12 and 20 ( $n = 3$ , \*  $p < 0.05$ ; day 0 was compared to the rest of the groups). (C) Live/dead assay performed on TEBV with HUVEC at 24 h and day 20. Live cells (green) and dead cells (red).

forming a monolayer, whereas HASMC remained with a round morphology (figures 10(A) and (B)). It is important to note that both cell types remained in their respective cell layers. Short after, cell tracker fluorescence decayed, not allowing imaging and performing the 3D reconstruction with confocal microscope.

#### 4. Discussion

In order to bioengineer blood vessels *in vitro*, it is important to reproduce their native architecture to obtain a proper function once cells are embedded. In this study, we have developed a stable TEBV through an extrusion technique. This structure was composed,



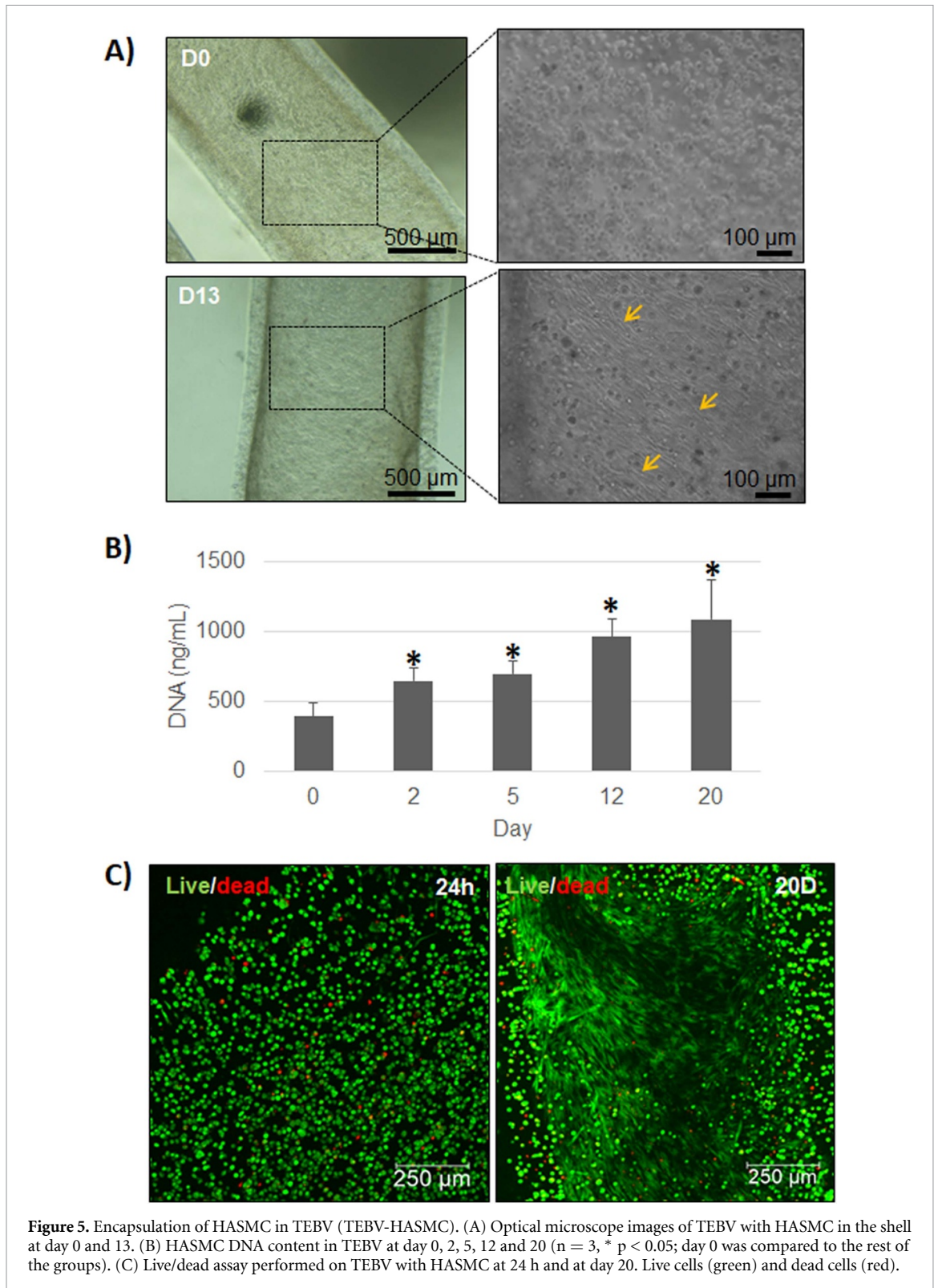
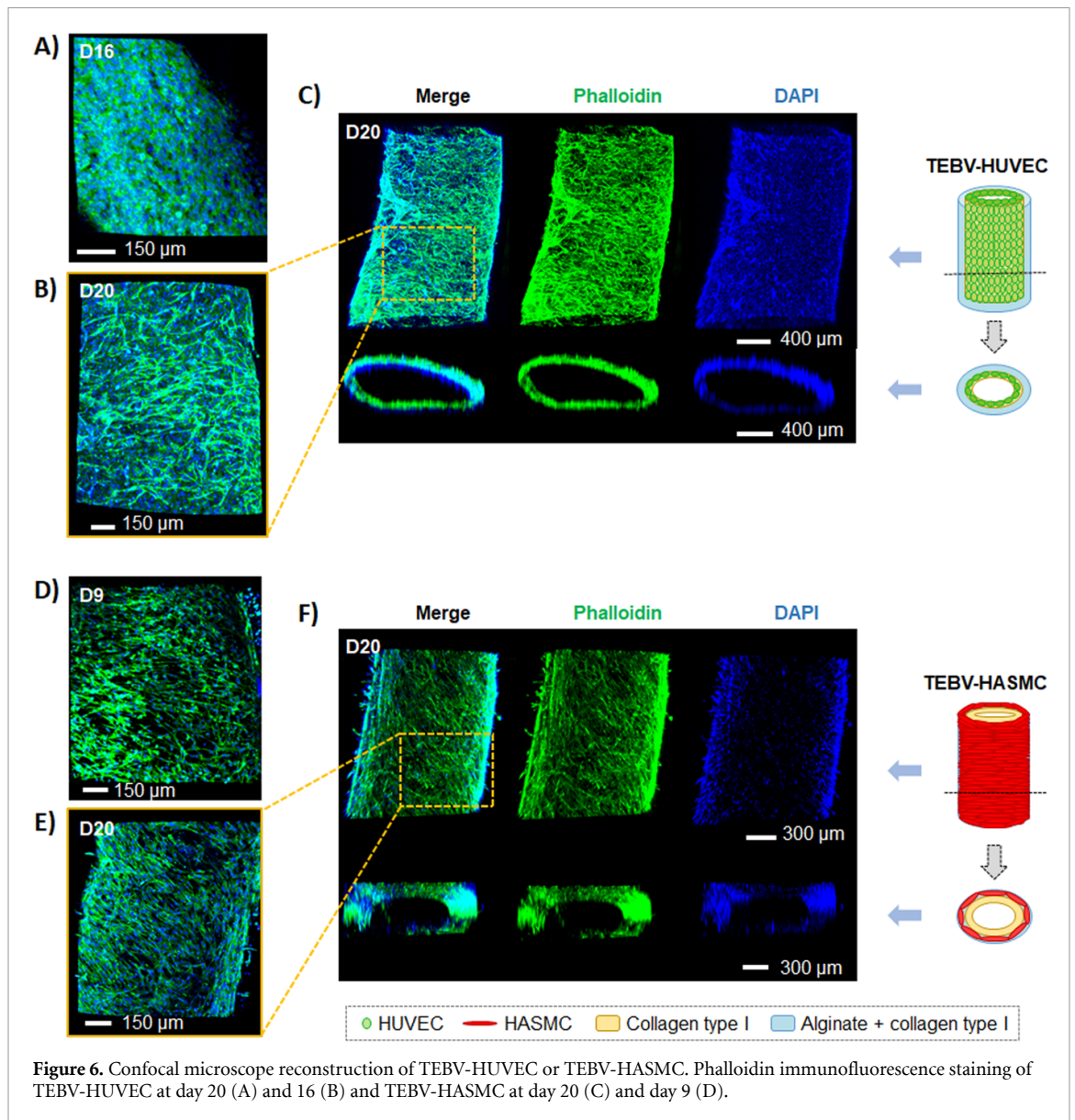


**Figure 5.** Encapsulation of HASMC in TEBV (TEBV-HASMC). (A) Optical microscope images of TEBV with HASMC in the shell at day 0 and 13. (B) HASMC DNA content in TEBV at day 0, 2, 5, 12 and 20 ( $n = 3$ , \*  $p < 0.05$ ; day 0 was compared to the rest of the groups). (C) Live/dead assay performed on TEBV with HASMC at 24 h and at day 20. Live cells (green) and dead cells (red).

from inside to outside, by a hollowed layer followed by a layer of collagen sheathed by an outer layer made of alginate and collagen. Due to the property of alginate to instantly crosslink when being in contact with divalent ions [28], an alginate solution could maintain the tubular structure when extruded within a calcium chloride. Moreover, Pluronic was able to gel at 37  $^{\circ}\text{C}$  [29] and it could maintain collagen into a tubular structure until it was gelled. When Pluronic

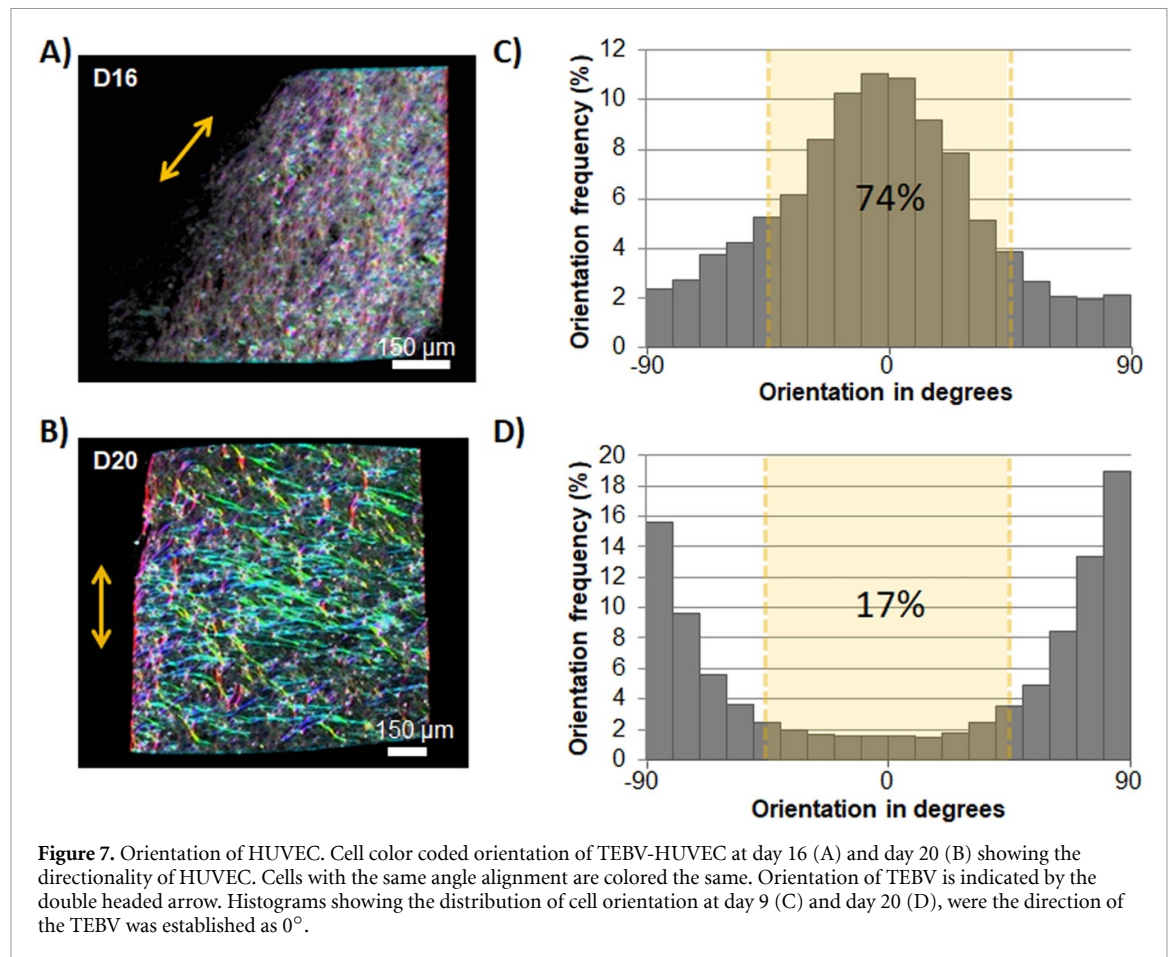
was removed from the inner core by dissolution, a stable dual-layered hollow construct was obtained.

A part from reproducing the architecture of a blood vessel, another important characteristic to take into account is the biomaterials used. Two of the major components of an artery are collagen and elastin. More specifically, the most prevalent extracellular matrix (ECM) protein is collagen, specially type I, distributed in all three tunica (intima, media and



adventitia) [30]. For this reason, predominantly collagen type I was used to develop our TEBV. When testing which concentration of collagen type I provided the maximum tubular stability in the inner layer, we found that  $5 \text{ mg ml}^{-1}$  was the optimum condition, as shown in figure 2(A). A part from collagen, alginate was elected as the main component for the outer layer to give stability to our TEBV, which we previously showed to be an interesting hydrogel for core shell fiber formation. Nevertheless, the absence of functional domains could prevent HASMCs stretching and hence was combined with collagen. A final concentration of 2% alginate was chosen, which conferred stability to our TEBV once it was extruded in calcium chloride solution (see supplementary information—video 1), and  $3 \text{ mg ml}^{-1}$  of collagen on the outer layer, in which it could be observed HASMC lengthening (figures 5(A) and supplementary information—figure 3).

An interesting feature of the extrusion method used in the present work was that TEBV diameters obtained were dependent to the injection speed, obtaining higher calibers with higher injections speeds, as well as higher wall thickness. With  $50 \text{ ml h}^{-1}$  the outer diameter was around  $1700 \mu\text{m}$  and the inner diameter around  $1500 \mu\text{m}$ , whereas with  $25 \text{ ml h}^{-1}$  the outer and inner diameter were around  $1500$  and  $1300 \mu\text{m}$ , respectively. The obtained results are similar to our previous study where we could observe an increase of the shell width when using the extrusion method, although our previous structures were non-hollowed core-shell constructs [21]. These sizes correspond to the range of arteries, as they are described to be within  $100 \mu\text{m}$  to  $10 \text{ mm}$  [31]. Moreover, there was a lower coefficient of variation (less than 5%) for outer and inner diameter, indicating homogeneity between TEBV and a high reproducibility using this technique. Since the differences between the TEBV sizes extruded at  $25$  and  $50 \text{ ml h}^{-1}$

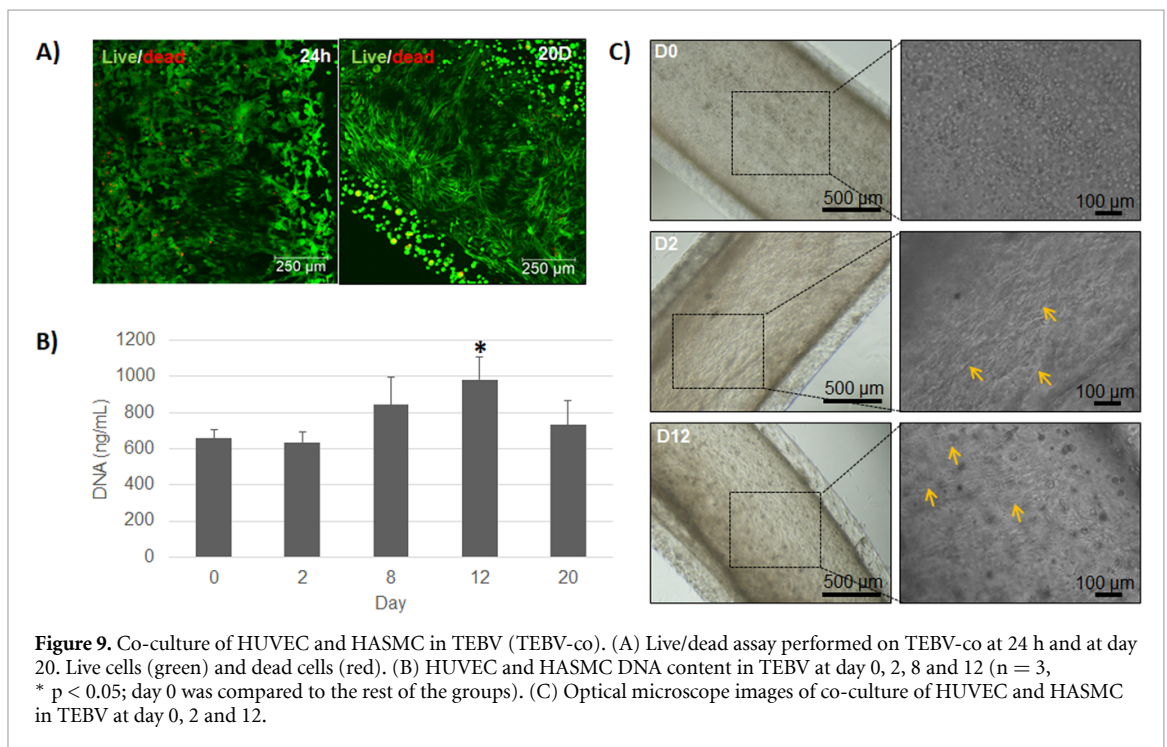
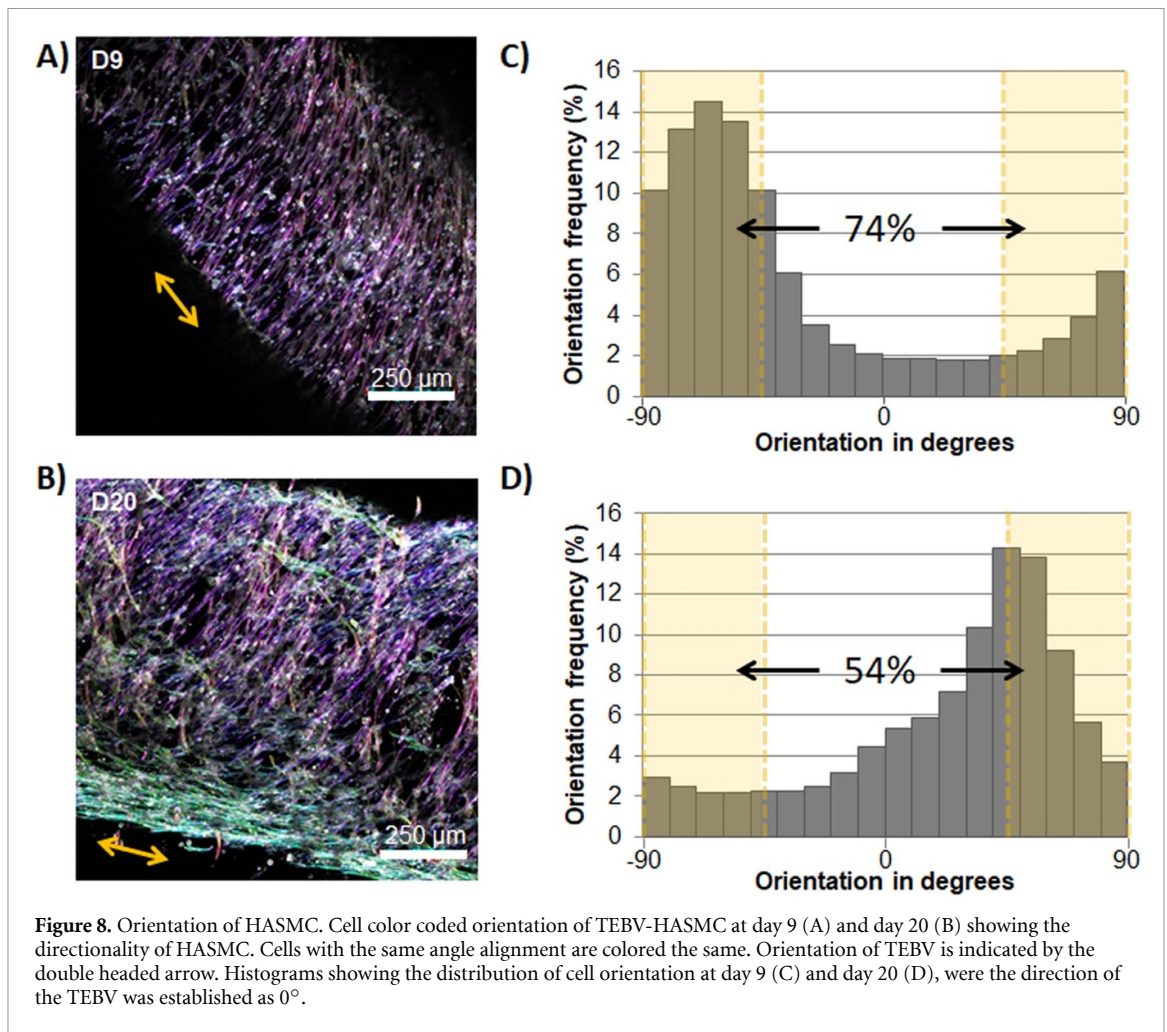


were very subtle, we decided to use the highest injection speed as it would take half the time to obtain the TEBV, hence increasing the chances of cell survival during extrusion process.

Due to the high injection speed chosen, we wanted to evaluate if cells could survive the shear stress suffered from the extrusion process at short time points. Furthermore, in order to guarantee nutrients and oxygen diffusion to the cells we also assessed cell survival at longer time points within the TEBV construct. We first encapsulated HUVEC in the inner layer (consisting of collagen) and HASMC in the outer layer (composed of alginate and collagen), in independent TEBV before performing a co-culture study. Both cell types exhibited high levels of viability during all time course of the experiment, being above 90% (figures 4(C) and 5(C)). These results suggest that the extrusion method was not harmful for these cells and they could survive within the TEBV construct. This is a positive result taking into account that the viability of cells using microextrusion bioprinting technique is described to be between 40 and 86% [32, 33]. Moreover, there was an increase of DNA content of HUVEC cells from day 2 compared to day 0 (figure 4(B)), suggesting that these cells had the proper 3D ECM conditions to proliferate. The content of DNA remained constant from day 2 to the end of experiment, implying that HUVEC

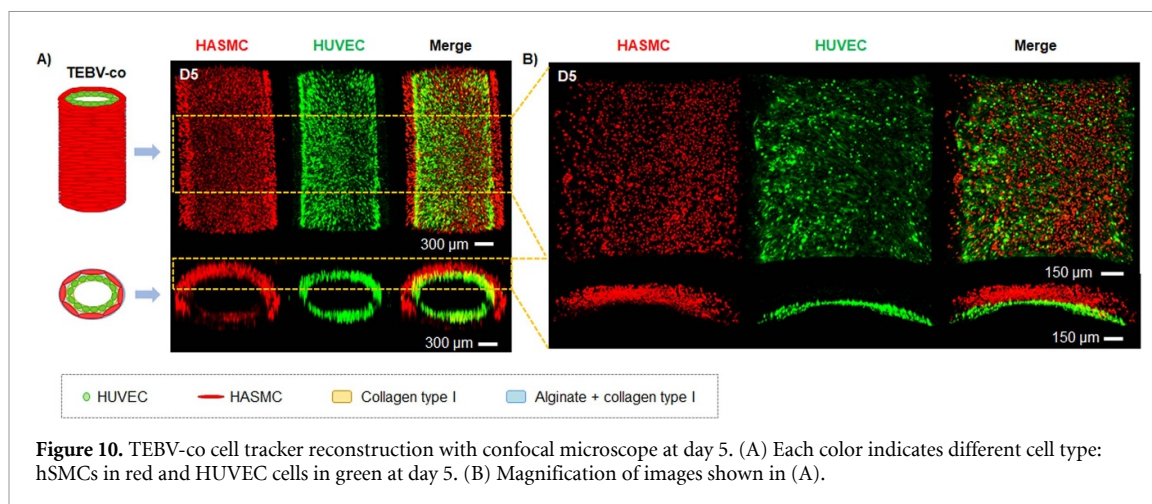
cells may have reached confluence in an early stage, probably due to the high amount of cells initially incorporated. With HASMC, a gradual and significant increase of DNA content was observed during the course of the experiment (figure 5(B)), suggesting that these cells also presented proper conditions to proliferate within TEBV structure. In this particular case, lower amounts of HASMC were loaded compared to HUVEC due the different cell size, being HASMC three times the size of HUVEC [25].

More interestingly, with F-actin staining, HUVEC were observed to be covering the entire inner tubular structure, forming a monolayer of cells at day 16 (figure 6(A)), although some cells grew over the monolayer at the end of experiment (figure 6(B)). A parallel alignment was also observed for HUVEC in TEBV during the initial days after extrusion (figure 4(A)) and persisted at day 16 (figures 7(A) and (C)) but this arrangement was not consistent at the end of TEBV culture (figures 6(B), (C) and 7(B), (D)). In physiological conditions, endothelial cells (EC) are submitted through a shear stress from the blood flow, which is described to induce the alignment of EC parallel to the vessel [22]. The extrusion method also applies a shear stress on the cells once they are extruded, and this could explain the initial parallel alignment of HUVEC. Because TEBV were cultured under static conditions, cells were not



exposed to a laminar flow shear stress and this could explain the loss of their parallel alignment at the

end of the experiment. A part from that, blood flow is needed to induce vessel maturation, which



leads the quiescence of ECs [34, 35], amongst others, and this would also explain why HUVEC cells kept reorganizing over the monolayer when they reached confluence.

Similarly, F-actin staining of HASMC, showed cells covering the outer layer of TEBV (figures 6(E) and (F)), having as well more cells at the end of the experiment compared with an early stage, such as day 9 (figure 6(D)), consistent with DNA content. More interestingly, the percentage of aligned cells between  $45^\circ$  and  $90^\circ$  (perpendicular arrangement) was 73% and 51% at day 9 and 20, respectively, suggesting a diagonal-perpendicular alignment of these cells resembling the perpendicular alignment found in native arterial blood vessels (figures 6(D)–(F) and 8(A)–(D) [10]. This alignment is consistent with previous reports showing that vascular smooth muscle cells aligns in a shear-stress-dependent manner, being their orientation perpendicular with low shear stress [36]. This alignment is of special interest as several mechanical functionalities of blood vessels, such as tensile strength, compliance and vasoactivity response, are mainly related to this conformation [37]. To our knowledge, this is the first time that HUVEC and HASMC can be aligned in a parallel and diagonal-perpendicular way without perfusion, respectively, without inducing a patterning modification to the biomaterial, as has been performed with other methodologies such as sheet rolling [13, 14] or electrospinning [38]. To our knowledge, the only study that also encapsulated HUVEC and HASMCs using triple co-axial nozzle did not achieved a native cell alignment in static conditions and could only achieved it after perfusion [20]. It is worth to mention that the collagen used was non-commercial and we isolated by ourselves. Although we demonstrated purity over 95%, as commercially available collagen solutions (see supplementary information-figure 1), we can not exclude the possibility of the presence of other bioactive factors within the collagen that might have helped to promote the perpendicular alignment of HASMCs.

Finally, after ensuring HUVEC and HASMC survival within the TEBV structure, we wanted to validate if they could behave in a similar way once they were co-cultured (TEBV-co). Cells exhibited a high percentage of viability as shown in figure 9(A), being above 90%, at 24 h and 20 d. These results suggest that both cell types could survive in co-culture within the TEBV construct, even at the end of the experiment where more cells were present. Optical microscope images (figure 9(C)) showed cell lengthening in the inner layer at day 2, and cell lengthening in the outer layer at day 12, although both cells types could not be distinguished. Because of this, each cell type was stained with specific cell tracker previous to TEBV development in order to distinguish them within the structure. In an early stage of cell culture, a monolayer of lengthened HUVEC cells was observed, whereas HASMC presented a round morphology (figures 10(A) and (B)). However, with the images obtained with the live/dead assay at 20 d we could observe that most of the cells were stretched (figure 9(A)). The differences in cell stretching could be related with the decreased content of collagen in the HASMC layer compared to the HUVEC layer. Further experiments are required to increase the collagen content in the outer layer to enhance cell-matrix interaction as well as perfusion culture, as it has been previously shown to induce to a greater extent the cell arrangement of HUVEC parallel to the flow and perpendicular arrangement of HASMC perpendicular to the flow [22, 39]. Nevertheless, it has to be taken into account that the presence of alginate is essential for the proper subsequent suturing of the TEBV and is the responsible for the stability after 20 d of culture. As we previously described, the concentration of alginate on the outer layer is responsible for an increased storage modulus, which was shown to have a dose dependent increase [21]. Moreover, it has been reported that perfusion of blood vessels also induces ECM deposition by HASMC [39, 40], further increasing their mechanical properties [41], and also enhance their maturation and functionality in terms of vasoactivity

and permeability [39, 42, 43]. Therefore, further studies should include perfusion of TEBVs and assessment of mechanical properties and functionality of these TEBVs.

## 5. Conclusions

In summary, it could be developed a TEBV-like structure in the range of arteries with this simple and low cost extrusion method in one step procedure, presenting high homogeneity between TEBV constructs leading to a high reproducibility of this technique. Moreover, it can be adapted to obtain TEBVs of higher caliber just changing the size of the triple concentric nozzle. The TEBVs obtained could be easily handled and can be potentially perfused. Furthermore, these TEBVs constructs were able to encapsulate HUVEC and HASMC, allowing their survival and proliferation within it. Additionally, HASMC showed a diagonal-perpendicular alignment, resembling the alignment of smooth muscle cells in native arterial blood vessels, whereas HUVEC cells presented parallel alignment. Further experiments are required using perfusion culture to maintain the proper cell alignment and induce maturation and functionality of the construct.

## Acknowledgments

This work was funded by the Government of Catalonia (2017 SGR 708), the Spanish Ministry (Ramón y Cajal fellowship (RYC2018-025977-I) and project RTI2018-096088-J-100 (MINECO/FEDER), and pre-doctoral fellowship from Universitat Internacional de Catalunya (UIC).

## ORCID iDs

E Bosch-Rué  <https://orcid.org/0000-0002-1131-4908>

Luis M Delgado  <https://orcid.org/0000-0001-7094-2966>

F Javier Gil  <https://orcid.org/0000-0003-3265-5071>

Roman A Perez  <https://orcid.org/0000-0002-0823-2303>

## References

- [1] World Health Organization 2017 Cardiovascular diseases (CVDs) (available at: [http://www.who.int/news-room/fact-sheets/detail/cardiovascular-diseases-\(cvds\)](http://www.who.int/news-room/fact-sheets/detail/cardiovascular-diseases-(cvds)))
- [2] Libby P et al 2019 Atherosclerosis *Nat. Rev. Dis. Primers* **5** 1–18
- [3] Chaabane C, Otsuka F, Virmani R and Bochaton-Piallat M L 2013 Biological responses in stented arteries *Cardiovasc. Res.* **99** 353–63
- [4] McKavanagh P, Zawadowski G, Ahmed N and Kutryk M 2018 The evolution of coronary stents *Expert Rev. Cardiovasc. Ther.* **16** 219–28
- [5] Kokkinidis D G, Waldo S W and Armstrong E J 2017 Treatment of coronary artery in-stent restenosis *Expert Rev. Cardiovasc. Ther.* **15** 191–202
- [6] Sabik J F 2011 Understanding saphenous vein graft patency *Circulation* **124** 273–5
- [7] Gu C X, Yang J F, Zhang H C, Wei H and Li L K 2012 Off-pump coronary artery bypass grafting using a bilateral internal mammary artery Y graft *J. Geriatr. Cardiol.* **9** 247–51
- [8] Rieder E, Steinacher-Nigisch A and Weigel G 2016 Human immune-cell response towards diverse xenogeneic and allogeneic decellularized biomaterials *Int. J. Surg.* **36** 347–51
- [9] Truskey G A 2010 Endothelial cell vascular smooth muscle cell co-culture assay for high throughput screening assays for discovery of anti-angiogenesis agents and other therapeutic molecules *Int. J. High Throughput Screen* **2010** 171–81
- [10] O'Connell M K, Murthy S, Phan S, Xu C, Buchanan J, Spilker R, Dalman R, Zarins C, Denk W and Taylor C 2008 The three-dimensional micro- and nanostructure of the aortic medial lamellar unit measured using 3D confocal & electron microscopy imaging *Matrix Biol.* **27** 171–81
- [11] McClelland M T and Stupp S 2013 Tubular hydrogels of circumferentially aligned nanofibers to encapsulate and orient vascular cells *Biomaterials* **33** 5713–22
- [12] Jung Y, Ji H, Chen Z, Fai Chan H, Atchison L, Klitzman B, Truskey G and Leong K W 2015 Scaffold-free, human mesenchymal stem cell-based tissue engineered blood vessels *Sci. Rep.* **5** 1–9
- [13] Yuan B, Jin Y, Sun Y, Wang D, Sun J, Wang Z, Zhang W and Jiang X 2012 A strategy for depositing different types of cells in three dimensions to mimic tubular structures in tissues *Adv. Mater. Weinheim* **24** 890–6
- [14] Chen M, Li L, Xia L, Zhang F, Jiang S, Hu H, Li X and Wang H 2020 Temperature responsive shape-memory scaffolds with circumferentially aligned nanofibers for guiding smooth muscle cell behavior *Macromol. Biosci.* **20** 1–11
- [15] Horakova J, Mikes P, Lukas D, Saman A, Jencova V and Klapstova A 2018 Electrospun vascular grafts fabricated from poly (L-lactide-co-ε-caprolactone) used as a bypass for the rabbit carotid artery Electrospun vascular grafts fabricated from poly (L-lactide-co-ε-caprolactone) used as a bypass for the rabbit carotid *Biomed. Mater.* **13** 065009
- [16] Higgins S P, Solan A K and Niklason L E 2003 Effects of polyglycolic acid on porcine smooth muscle cell growth and differentiation *J. Biomed. Mater. Res. A* **67** 295–302
- [17] Gao G et al 2017 Tissue engineered bio-blood-vessels constructed using a tissue-specific bioink and 3D coaxial cell printing technique: a novel therapy for ischemic disease *Adv. Funct. Mater.* **27** 1–12
- [18] Onoe H et al 2013 Metre-long cell-laden microfibrils exhibit tissue morphologies and functions *Nat. Mater.* **12** 584–90
- [19] Zhang Y, Yu Y, Akkouch A, Dababneh A, Dolati F and Ozbolat I T 2015 In vitro study of directly bioprinted perfusable vasculature conduits *Biomater. Sci.* **3** 134–43
- [20] Gao G et al 2019 Tissue-engineering of vascular grafts containing endothelium and smooth-muscle using triple-coaxial cell printing *Appl. Phys. Rev.* **6** 4
- [21] Perez R A, Kim M, Kim T H, Kim J H, Lee J H, Park J H, Knowles J C and Kim H-W 2014 Utilizing core-shell fibrous collagen-alginate hydrogel cell delivery system for bone tissue engineering *Tissue Eng. A* **20** 103–14
- [22] Li Y, Huang G, Zhang X, Wang L, Du Y, Lu T J and Xu F 2014 Engineering cell alignment in vitro *Biotechnol. Adv.* **32** 347–65
- [23] Deng X et al 2013 Biomechanical regulation of vascular smooth muscle cell functions: from in vitro to in vivo understanding *J. R. Soc. Interface* **11** 20130852–20130852
- [24] Delgado L M, Shologu N, Fuller K and Zeugolis D I 2017 Acetic acid and pepsin result in high yield, high purity and

- low macrophage response collagen for biomedical applications *Biomed. Mater.* **12** 65009
- [25] Heydarkhan-Hagvall S, Helenius G, Johansson B R, Li J Y, Mattsson E and Risberg B 2003 Co-culture of endothelial cells and smooth muscle cells affects gene expression of angiogenic factors *J. Cell. Biochem.* **89** 1250–9
- [26] Gui L et al 2016 Implantable tissue-engineered blood vessels from human induced pluripotent stem cells *Biomaterials* **102** 120–9
- [27] Mohammed M, Thurgood P, Gilliam C, Nguyen N, Pirogova E, Peter K, Khoshmanesh K and Baratchi S 2019 Studying the response of aortic endothelial cells under pulsatile flow using a compact microfluidic system *Anal. Chem.* **91** 12077–84
- [28] Lee K Y and Mooney D J 2012 Alginate: properties and biomedical applications *Prog. Polym. Sci.* **37** 106–26
- [29] Goffredi E, Boffito M, Calzone S, Giannitelli S M, Rainer A, Trombetta M, Mozetic P and Chiono V 2016 Pluronic F127 hydrogel characterization and biofabrication in cellularized constructs for tissue engineering applications *Procedia CIRP* **49** 125–32
- [30] Miranda-Nieves D and Chaikof E L 2017 Collagen and elastin biomaterials for the fabrication of engineered living tissues *ACS Biomater. Sci. Eng.* **3** 694–711
- [31] Baker G F, Tortora G J and Nostalos N P A 2006 Principles of anatomy and physiology *Am. J. Nurs.* **76** 477
- [32] Bishop E S, Mostafa S, Pakvasa M, Luu H H, Lee M J, Moriatis J, Ameer G A, He T-C and Reid R R 2017 3-D bioprinting technologies in tissue engineering and regenerative medicine : current and future trends *Genes Dis.* **4** 185–95
- [33] Chang R, Nam J A E and Sun W E I 2008 Effects of dispensing pressure and nozzle diameter on cell survival from solid freeform fabrication - based direct cell writing *Tissue Eng. A* **14** 41–48
- [34] Carmeliet P and Jain R K 2011 Molecular mechanisms and clinical applications of angiogenesis *Nature* **473** 298–307
- [35] Paszkowiak J J and Dardik A 2003 Arterial wall shear stress: observations from the bench to the bedside *Vasc. Endovascular Surg.* **37** 47–57
- [36] Qiu J, Zheng Y, Hu J, Liao D, Gregersen H, Deng X, Fan Y and Wang G 2014 Biomechanical regulation of vascular smooth muscle cell functions : from in vitro to in vivo understanding *J. R. Soc. Interface* **11** 90
- [37] Chan-Park M B, Shen J Y, Cao Y, Xiong Y, Liu Y, Rayatpisheh S, Kang G C-W and Greisler H P 2009 Biomimetic control of vascular smooth muscle cell morphology and phenotype for functional tissue-engineered small-diameter blood vessels *J. Biomed. Mater. Res. A* **88** 1104–21
- [38] Wu T, Zhang J, Wang Y, Li D, Sun B, El-Hamshary H, Yin M and Mo X 2018 Fabrication and preliminary study of a biomimetic tri-layer tubular graft based on fibers and fiber yarns for vascular tissue engineering *Mater. Sci. Eng. C* **82** 121–9
- [39] Eoh J H, Shen N, Burke J A, Hinderer S, Xia Z, Schenke-layland K and Gerecht S 2017 Enhanced elastin synthesis and maturation in human vascular smooth muscle tissue derived from induced-pluripotent stem cells *Acta Biomater.* **52** 49–59
- [40] Oikonomou E, Tsalamandris S, Mourouzis K and Tousoulis D 2017 Biology of the vessel wall *Coronary Artery Disease* (Amsterdam: Elsevier) pp 3–12
- [41] Fernandez C E, Yen R W, Perez S M, Bedell H W, Povsic T J, Reichert W M and Truskey G A 2016 Human vascular microphysiological system for in vitro drug screening *Sci. Rep.* **6** 21579
- [42] Price G M, Wong K H K, Truslow J G, Leung A D and Tien J 2011 Effect of mechanical factors on the function of engineered human blood microvessels in microfluidic collagen gels *Biomaterials* **31** 6182–9
- [43] Ando J and Yamamoto K 2011 Effects of shear stress and stretch on endothelial function *Antioxid. Redox Signaling* **15** 1389–403